

Effect of a Quaternary Ammonium Salt on Propylene Carbonate Structure in Slit-Shape Carbon Nanopores

Akimi Tanaka,[†] Taku Iiyama,[‡] Tomonori Ohba,[†] Sumio Ozeki,[‡] Koki Urita,[†] Toshihiko Fujimori,[†] Hirofumi Kanoh,[†] and Katsumi Kaneko^{*,†}

Department of Chemistry, Graduate School of Science, Chiba University, 1-33 Yayoi-cho, Inage-ku, Chiba 263-8522, Japan, and Department of Chemistry, Faculty of Science, Shinshu University, 3-1-1, Asahi, Matsumoto, Nagano 390-8621, Japan

Received October 15, 2009; E-mail: kaneko@pchem2.s.chiba-u.ac.jp

An electrical double-layer capacitor (EDLC) with nanoporous carbons as large-area electrodes is one of the key devices indispensable to clean energy technology. Many scientists and engineers have attempted to develop EDLCs exhibiting better performance. Researchers from various fields of chemistry have been studying EDLCs.^{1,2} An electrical double layer (EDL) plays an essential role in governing colloid stability. A charged particle is surrounded by oppositely charged ions to form an EDL, stabilizing the dispersion.² The thickness of the EDL formed on a colloid surface is believed to be less than 1 nm, which roughly corresponds to the pore width of the carbon electrodes of the EDLC, although the EDL structure is not well understood. Thus, it is necessary to examine the ionic solution structure in carbon nanopores. In our previous studies, we elucidated that molecules such as those of water, SO₂, alcohols, etc.³ that are confined in carbon nanopores, form a highly ordered structure, and a high-pressure gas-phase reaction occurs in the carbon nanopores without the application of a high pressure of 100 MPa order, which is generally required in the bulk gas phase.⁴ The partial dehydration of Rb⁺ and Ca²⁺ ions by confinement in carbon nanopores was evidenced by EXAFS and simulation techniques.⁵ Chmiola et al. found that nanoporous carbide-derived carbon with a pore width <1 nm showed a remarkable efficiency in storing electrical charges, even in the case of organic salt solutions.⁶ The purpose of the present study is to elucidate the structure of an electrolytic solution confined in 1-nm-wide carbon nanopores. Further developments in EDLCs require a fundamental understanding of the structure of an organic electrolytic solution formed in 1-nm-wide carbon nanopores. This Communication describes the effect of addition of tetraethylammonium tetrafluoroborate (Et₄NBF₄) on the structure of propylene carbonate (PC) confined in slit-shaped carbon nanopores of activated carbon fiber, which was studied by use of synchrotron X-ray diffraction (XRD) and reverse Monte Carlo (RMC) simulation.

Pitch-based activated carbon fiber (ACF) was used after grinding in an agate mortar. The surface area, micropore volume, and average slit-pore width were measured to be 1500 m² g⁻¹, 0.73 mL g⁻¹, and 1.0 nm, respectively, according to N₂ adsorption at 77 K by the subtracting pore effect method.⁷ ACF was pretreated at 393 K and 1 mPa for 2 h, and then it was immersed in 0.5 and 1.0 M Et₄NBF₄-PC solutions in order to introduce those solutions in pores. The PC and Et₄NBF₄ solutions deposited on the external surface of ACF were evaporated at 373 K for 3 h under a flow of N₂ (200 mL min⁻¹), and thereby the residual amount of PC or Et₄NBF₄-PC solutions on the external surface of ACF was less than 5% of the amount in the nanopores, as found from a thermal gravimetric analysis (see Supporting Information, S2–3).

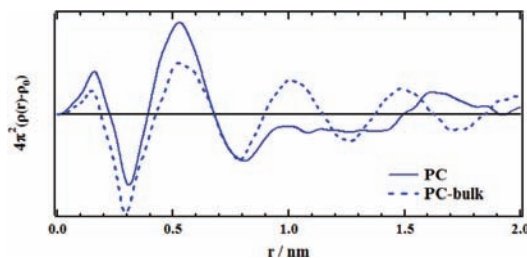


Figure 1. Electron radial distribution functions of bulk PC and PC confined in the carbon nanopores.

The RMC simulation was carried out using the XRD data and the probable molecular arrangement was deduced, which agreed with experimental XRD data obtained on molecules adsorbed in the nanopores.⁸ The XRD pattern of the adsorbed molecules was determined by the correction procedure (the detailed procedure is given in Supporting Information, S4–8). A slit-shaped carbon model consisting of double graphene sheets was used for the simulation. A new configuration was generated in an RMC trial that was randomly chosen by moving (including rotation), inserting, and deleting a molecule. The ratio of the number of molecules of Et₄N, BF₄, and PC was fixed in the calculation. The RMC simulation was repeated over 5 000 000 steps until there was no more improvement in the fitting between the simulation results and the experimental data. In the RMC, the atomic configuration of molecules in the pore was optimized, and no molecular structural distortion was assumed.

The synchrotron XRD patterns of ACF and PC-adsorbed ACF showed three broad peaks around 15°, 28°, and 50°, which were assigned to (002), (100) and (101), and (110) lattices of the graphitic structure of ACF (see Supporting Information, S9). The peaks of PC-adsorbed ACF shifted to a smaller angle. The small-angle X-ray scattering, scatterings from molecules and carbon walls, and carbon-carbon interference scattering were experimentally corrected. The molecule-molecule and the molecule-carbon wall interference scatterings, which provided the electron radial distribution functions (ERDFs) for confined molecules, were determined by the correction procedure (see Supporting Information, S4–7). Figure 1 shows the ERDFs of PC in the bulk liquid phase and PC confined in the nanopores. The ERDFs were obtained by calculating the inverse Fourier transform of the structure function from the corrected XRD patterns. The positive peaks around 0.15 and 0.5 nm are attributed to the intramolecular structure and the nearest-neighbor PC molecules, respectively. The intensity of this nearest-neighbor peak of confined PC is larger than that of the bulk liquid PC. The ERDF of adsorbed PC shows no clear peaks above 0.8 nm, but that of bulk PC shows two additional peaks. It implies

[†] Chiba University.

[‡] Shinshu University.

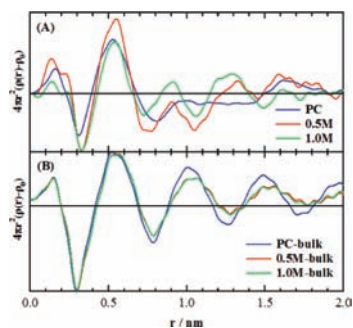


Figure 2. ERDFs of confined (A) and bulk (B) Et_4NBF_4 -PC solutions at 303 K.

that the number of the nearest-neighbor PC molecules confined in the nanopores is relatively larger than that in bulk PC, and the PC molecules cannot form a long-range ordered structure due to an intensive restriction effect. Figure 2 shows the ERDFs of the confined and bulk Et_4NBF_4 -PC solutions measured at 303 K. All the nearest-neighbor peaks of the bulk PC solutions are similar to each other, and only slight changes are observed in the vicinity of the second- and third-nearest-neighbor peaks upon addition of the salts. On the other hand, the addition of the salts results in a dramatic change in the nearest-neighbor peak of PC confined in the nanopores. In particular, beyond the second-nearest-neighbor peak, the structure varies considerably as a result of the addition of the salts. Pure PC adsorbed in the pores shows no peaks around 1 nm, while the addition of the salts leads to distinct double peaks in the range from 0.7 to 1.3 nm. Thus, the addition of the salts induces a distinct ordering of the PC molecules in the carbon nanopores.

This phenomenon of ordering is more explicitly understood from the structural images obtained from the RMC simulation, as shown in Figure 3. The agreement between the experimental and simulated XRD patterns of PC and Et_4NBF_4 -PC solutions confined in the slit-shaped graphite pores is discussed in Supporting Information, S10–11. PC molecules are closely packed in the pore without an explicit ordering from the snapshot in the absence of the salts. The distribution of PC molecules along the pore width is quite uniform, as shown in Figure 3A. This uniform distribution coincides with the previous ERDF results. The addition of the salts gives rise to considerable variations in the distribution of the PC molecules: the distribution has double peaks near the monolayer positions on the both pore walls. Thus, the addition of Et_4NBF_4 electrolytes promoted the orientation of the PC molecules along the pore walls. This also agrees with the ordering feature in the ERDF shown in Figure 2. The snapshot strongly suggests that PC molecules form a double-layer-like structure by including tetraethylammonium and tetrafluoroborate ions. It is noteworthy that PC molecules vary their confined solution structure to accept the organic salts efficiently regardless of the intensive space restriction. This structural modulation function of PC molecular assemblies should contribute to the evolution of high capacitance in the carbon nanopores. Future studies are needed to establish the relationship between the pore width and accumulated ionic structure.

Acknowledgment. This work was partially supported by a Grant-Aid for Scientific Research (A) (No. 21241026) from the Japan Society for the Promotion of Science. The synchrotron

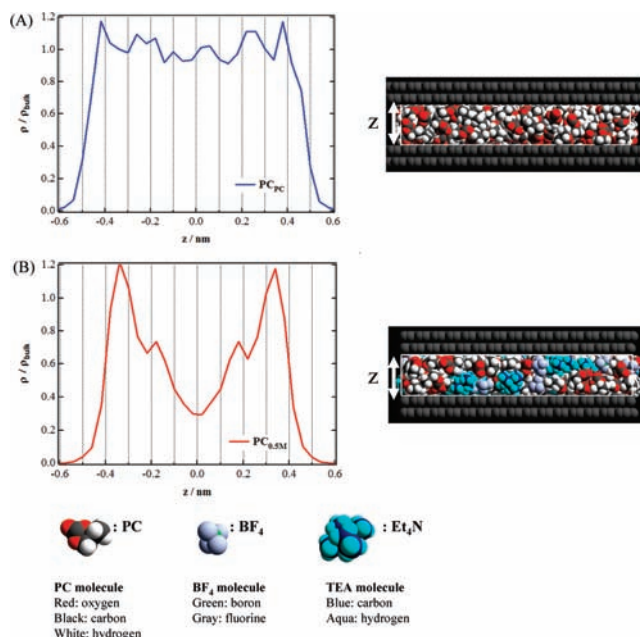


Figure 3. Snapshots and distribution of PC molecules and electrolytes along the pore width. (A) Pure PC; (B) Et_4NBF_4 -PC solution corresponding to 0.5 M bulk solution. The coordinate z along the pore width is shown by an arrow.

radiation experiments were performed at SPring-8 with the approval of the Japan Synchrotron Radiation Research Institute (JASRI) as part of the Nanotechnology Support Project of the Ministry of Education, Culture, Sports, Science and Technology, Japan.

Supporting Information Available: TG curves of PC and electrolyte-PC ACF, synchrotron XRD patterns before and after correction, and agreement of the experimental and reverse Monte Carlo simulated XRD patterns. This material is available free of charge via the Internet at <http://pubs.acs.org>.

References

- (a) Simon, P.; Gogotsi, Y. *Nat. Mater.* **2008**, *7*, 845–854. (b) Zhang, L. L.; Zhao, X. S. *Chem. Soc. Rev.* **2009**, *38*, 2520–2531.
- (a) Wernersson, E.; Kjellander, R. *J. Phys. Chem. B* **2007**, *111*, 14279–14282. (b) Stjepan, M. *J. Phys. Chem. B* **2006**, *110*, 13062–13067.
- (a) Wang, Z. M.; Kaneko, K. *J. Phys. Chem.* **1995**, *99*, 16714–16721. (b) Iiyama, T.; Nishikawa, K.; Otowa, T.; Kaneko, K. *J. Phys. Chem.* **1995**, *99*, 10075–10076. (c) Ohkubo, T.; Iiyama, T.; Nishikawa, K.; Suzuki, T.; Kaneko, K. *J. Phys. Chem. B* **1999**, *103*, 1859–1863.
- (a) Imai, J.; Souma, M.; Ozeki, S.; Suzuki, T.; Kaneko, K. *J. Phys. Chem.* **1991**, *95*, 9955–9960. (b) Yamamoto, T.; Tryk, D. A.; Hashimoto, K.; Fujishima, A.; Okawa, M. *J. Electrochem. Soc.* **2000**, *147*, 3393–3400. (c) Santiso, E. E.; Kostov, M. K.; George, A. M.; Nardelli, M. B.; Gubbins, K. E. *Appl. Surf. Sci.* **2007**, *253*, 5570–5579.
- (a) Ohkubo, T.; Konishi, T.; Hattori, Y.; Kanoh, H.; Fujikawa, T.; Kaneko, K. *J. Am. Chem. Soc.* **2002**, *124*, 11860–11861. (b) Ohkubo, T.; Hattori, Y.; Kanoh, H.; Konishi, T.; Fujikawa, T.; Kaneko, K. *J. Phys. Chem. B* **2003**, *107*, 13616–13622. (c) Ohba, T.; Kojima, N.; Kanoh, H.; Kaneko, K. *J. Phys. Chem. C* **2009**, *113*, 12622–12624.
- (a) Chmiola, J.; Yushin, G.; Gogotsi, Y.; Portet, C.; Simon, P.; Taberna, P. L. *Science* **2006**, *313*, 1760–1763. (b) Chmiola, J.; Largeot, C.; Taberna, P. L.; Simon, P.; Gogotsi, Y. *Angew. Chem., Int. Ed.* **2008**, *47*, 3392–3395.
- Setoyama, N.; Suzuki, T.; Kaneko, K. *Carbon* **1998**, *36*, 1459–1467.
- (a) Chialvo, A. A. *J. Chem. Phys.* **1990**, *92*, 673. (b) McGreevy, R. L.; Pusztai, L. *Mol. Simul.* **1988**, *1*, 359–367. (c) Iiyama, T.; Hagi, K.; Urushibara, T.; Ozeki, S. *Colloids Surf. A* **2009**, *347*, 133–141.

JA9087874